8th European Workshop On Structural Health Monitoring (EWSHM 2016), 5-8 July 2016, Spain, Bilbao
www.ndt.net/app.EWSHM2016

A Linearized Impact Localization Algorithm for the Health Monitoring of Aerospace Components

Mario Emanuele DE SIMONE, Salvatore BOCCARDI, Francesco CIAMPA*, Michele MEO
Mechanical Engineering Department, University of Bath, Bath, United Kingdom

*email: f.ciampa@bath.ac.uk

Key words: Impact Localization, acoustic emission, guided wave propagation.

Abstract

Literature presents a wide range of techniques and algorithms for the localization of impact source in isotropic structures. However, many of these methods involve either solving complex systems of nonlinear equations or a-priori training of the monitored structure. This is not only time consuming, but it requires high levels of computational effort that may often result in a poor estimation of the impact coordinates. This paper presents a novel structural health monitoring system for the impact localization on aluminium components. The proposed methodology, in contrast to current impact localization techniques, relies on an optimal sensor placement, which allows reducing the nonlinear system of equations to a linearized and simplified form. Two different Akaike Information Criterion (AIC) pickers are used to calculate the arrival times of the direct elastic waves originated by the impact source. To validate this methodology, experimental tests were carried out on aerospace components using four surface-bonded piezoelectric sensors. The results showed that this technique allows detecting and localizing the impact source with a high level of accuracy in any point of the structure.

1 INTRODUCTION

Real-time acoustic emission (AE) source localization is crucial in both non-destructive evaluation (NDE) and structural health monitoring (SHM) systems. Most of previous works about impact localization were based on the triangulation technique (also known as the Tobias algorithm), wherein the impact point is identified as the intersection of three circles, whose centers are the sensors location [1]. The main issue with this method is that it is suitable only for isotropic media for which the wave group velocity is known and remains the same in all directions. However, this is not true in the case of anisotropic and inhomogeneous materials as well as for dispersive guided waves in which the wave velocity is not constant, but it is a function of the frequency.

This paper is a follow-up of the work from Ciampa and Meo [2] based on (i) the resolution of a set of nonlinear equations for finding the coordinates of an impact source and (ii) the knowledge of time differences of arrival (TDOAs) calculated from time of arrivals (TOAs) by using the magnitude of the Continuous Wavelet Transform (CWT) squared modulus. The proposed new algorithm, is based on a linearization of the previous algorithm [2] and on TOAs values calculated by the Akaike Information Criterion (AIC). The advantages of this novel methodology are the simplicity and higher accuracy of the linearized approach and the higher precision of AIC methods [3] in comparison to the Wavelet Transform.

The ToA is the crucial parameter to be determined in an impact localization algorithm, since a TDOA is calculated as the simple difference between ToAs of two signals. ToA can be considered as the onset time of a signal generated by an impact source, so that a method able to identify this value with great accuracy in necessary. Usually, the onset time is usually picked as the point where the first difference between the signal and noise takes place [4]. A great number of algorithms for automatic detection of onset times were proposed in the last few years [11][5], many of them modified from seismology [6-8] due to similarities between research fields. Among them, two methods based on Akaike Information Criterion [5] will be investigated in this paper.

2 AKAIKE INFORMATION CRITERION

A sophisticated approach for onset time determination is to model a signal as an autoregressive (AR) process. The main idea is that the non-informative part (noise) and the informative part (signal) of a time series could be considered as two locally stationary processes, where the ToA is present. AIC is defined as following equation:

$$AIC = -2\ln(L) + 2P \tag{1}$$

where P is the number of parameters in the statistical model, and L is the maximized value of the likelihood function for the estimated model. Originally, (1) was designed to determine the optimal order for an AR process fitting a time series. In our case, the order of the AR process is fixed, so the AIC function is a measure for the model fit. The k separation point between noise and signal is identified as the point where the AIC is minimized and this is regarded as the onset time. The described approach, known as AR-AIC picker, has been used in seismology [6]. In the proposed methodology for the ToA, the following AIC function was used [9]:

$$AIC(k) = k\log\big(var(x[1,k])\big) + (N-k-1)\log(var(x[k+1,N])) \tag{2}$$

where x is the time serie of length N, k is the range through all signal points, $var(x[1,k])$ is the variance of the corresponding interval from 1 to k of signal x, while $var(x[k+1,N])$ means that all samples ranging from $k+1$ to N are considered. The AIC global minimum corresponds with the ToA. It should be noted that in AIC minimum calculation, it is not necessary to consider the whole time series but only the chosen window containing the onset time. Therefore the choice of the proper time window is crucial for the performance of AIC picker.

3 TWO-STEP AIC PICKER – METHOD 1

3.1 Characteristic function

The first considered method is a two-step AIC picker [3], based on the AIC function and a particular mathematical function called "characteristic" function (CF). It is possible to detect the arrival time through a change in the frequency, or amplitude, or both, in the time series. The purpose of a characteristic function is to enhance this change, by improving the resolution levels between noise and signal. A number of characteristic functions was here proposed: i.e. the absolute value function $CF(i) = |x(i)|$, the envelope of the signal calculated by the Hilbert transform, the square function $CF(i) = x(i)^2$ and the squared envelope. The last two functions enhance the amplitude changes but are not sensitive to periodic signal variations. Allen used a squared polynomial function [10], limited by the fact that it can suppress the amplitude of weaker modes, so it is suitable for bulk specimens and it is not effective in thin plates.
For signals with low signal-to-noise ratio, the following function was used:

$$CF(i) = |x(i)| + R|x(i) - x(i-1)| \tag{3}$$

where R is a constant set to $R = 4$ for thin-plate specimens in accordance to [3].

3.2 Algorithm

This first algorithm for the ToA estimation is a two-step process. The first step consists of calculating the characteristic function (3) for the measured signals, determining the shortened time window, and applying the AIC picker on the new time window.

The main assumption is that the time window starts within the noise level and ends just after the maximum amplitude value of the signal. So the starting time was set at the beginning of the original signal (considered a non-informative part), and the ending time was set after the maximum value of the characteristic function on time $t_{MAX} + \Delta t_{AM}$. t_{MAX} is the time of the global maximum of CF and the time delay Δt_{AM} is a value depending on the tested material that for our experiment was set to $20\ \mu s$.

The AIC picker based on (2), considering the CF function instead of the raw signal, is applied on this time window. The global minimum of the AIC function determines the first estimation of the onset time.

The second step allows improving the accuracy of ToA for the method developed in the first step by focusing on the neighborhood of the first estimation. The AIC picker applied on CF operates in a new and shortened time window, whose starting is at Δt_{FB} before the first estimation calculated at the end of first step, and the end is at Δt_{FA} after the first estimation. Similarly to Δt_{AM}, these two new values were set to $\Delta t_{FA} = 10\ \mu s$ and $\Delta t_{FB} = 30\ \mu s$. The global minimum of the recalculated AIC function defines the actual ToA.

4 TWO-STEP AIC PICKER – METHOD 2

4.1 Algorithm

The second method for the ToAs estimation is a two-step AIC picker [11] based on the AIC function, which does not use any characteristic function.

As mentioned before, the quality of an AIC picker improves if it is applied on a pre-selected time window containing the onset time [8]. The first step starts with the determination of a shortened time window by a method using a threshold amplitude level:

$$\sum_{i=k+1}^{10} |x(i)| \Big/ 10 \geq 4\left(\sum_{i=1}^{k} |x(i)|\right) \Big/ k \tag{4}$$

The threshold level was set by comparing the mean amplitude of a shifting set of 10 data and the fourfold mean amplitude of the interval of the time series ranging from1 to k is made. The pre-determined onset time (k_0) is calculated as the first value of k which satisfies (4).

Then the AIC picker based on (2) is applied to the time interval $[1, k_0]$ for a rough determination of the onset time k_1.

In the second step, the AIC picker acts on a new time window centered in k_1 with a length of $2\Delta k$, depending on the sample frequency. A variant of this method [12], also used in this work, considers a length of $2(k_1 - k_0)$. The k_{min} value, obtained from the application of the AIC picker to this time window is the actual ToA of the acquired signals.

5 LINEARIZED IMPACT LOCALIZATION ALGORITHM

For the determination of the impact localization coordinates, let us consider an impact source point I, at unknown coordinates (x_I, y_I) in the plane of the plate $x - y$, and a number of n receiver transducers located at distance d_i $(i = 1, \dots, n)$ from the source. The source coordinates can be determined by solving the following general system of nonlinear equations [2]:

$$\begin{cases} \|d_i\|^2 = (x_i - x_I)^2 + (y_i - y_I)^2 \\ t_i = \dfrac{\|d_i\|}{V_g} \end{cases} \tag{5}$$

where V_g is the velocity of propagation of the stress wave reaching the ith transducer, t_i is the time of detection of the acoustic emission signals and (x_i, y_i) are the coordinates of the ith sensor.

Combining both terms of (5) it is possible to obtain, for each sensor, the following equation:

$$(x_i - x_I)^2 + (y_i - y_I)^2 - \left(t_i V_{g,i}\right)^2 = 0 \tag{6}$$

that is the equation of a circumference with radius $r_i^2 = \left(t_i V_{g,i}\right)^2$. Choosing one of the sensors as reference sensor, it is possible to write:

$$t_j = t_{ref} + \Delta t_{ref,j} \tag{7}$$

where t_{ref} is the travel time necessary to reach the reference sensor and $\Delta t_{ref,j}$ are the time differences between sensor j and the reference one (i.e. $\Delta t_{ref,j} = t_j - t_{ref}$).

Substituting equation (7) into (6), it yields:

$$(x_i - x_I)^2 + (y_i - y_I)^2 - \left[\left(t_{ref} + \Delta t_{ref,j}\right)V_g\right]^2 = 0 \tag{8}$$

The above system consists of four unknowns $x = \{x_I, y_I, t_{ref}, V_g\}$. The input values are the sensors location and the $\Delta t_{ref,j}$ values, obtained from a difference between the ToAs calculated by using one of the two methods proposed in Sections 3 and 4.

5.1 Linearization of the set of nonlinear equations

In comparison to previous works [2], here the aim is to linearize the system (8) to avoid the use of both local (Newton's) and global (unconstrained optimization) methods for solving nonlinear equations. This would eliminate the dependence on the guess conditions for the solution of the nonlinear system of equations, thus improving the accuracy in the estimation of the impact coordinates. Assuming sensor number 1 as reference sensor, the set of nonlinear equations (5) is modified as follows:

$$\begin{cases} (x_i - x_I)^2 + (y_i - y_I)^2 - \left[\left(t_1 + \Delta t_{1,i}\right)V_g\right]^2 = 0 \\ (x_1 - x_I)^2 + (y_1 - y_I)^2 - \left(t_1 V_g\right)^2 = 0 \end{cases} \tag{9}$$

with $i = \{2, \dots, n\}$.

Subtracting the reference sensor equation from other equations, it is possible to obtain:

$$x_i^2 - x_1^2 - 2x_i x_I + 2x_1 x_I + y_i^2 - y_1^2 - 2y_i x_I + 2y_1 x_I - V_g^2 \Delta t_{1,i}\left(\Delta t_{1,i} + 2t_1\right) = 0 \tag{10}$$

Considering $b_i = (x_i + y_i)^2 - (x_1 + y_1)^2$, equations (10) become:

$$b_i - 2[x_I(x_i - x_1) + y_I(y_i - y_1)] - V_g^2 \Delta t_{1,i}\left(\Delta t_{1,i} + 2t_1\right) = 0 \tag{11}$$

Using the following positions, $x_{1,i} = x_i - x_1$ and $y_{1,i} = y_i - y_1$, it yields:

$$b_i - 2\left(x_I x_{1,i} + y_I y_{1,i}\right) - {V_g}^2 \Delta t_{1,i}\left(\Delta t_{1,i} + 2t_1\right) = 0 \tag{12}$$

Dividing by 2 and rearranging, equation (12) becomes:

$$x_I x_{1,i} + \; y_I y_{1,i} + {V_g}^2 t_1 \Delta t_{1,i} = \frac{b_i}{2} - {V_g}^2 \frac{{\Delta t_{1,i}}^2}{2} \tag{13}$$

With four sensors, the number of unknowns is equal to number of equations, so that in matrix form it is possible to write:

$$\begin{bmatrix} x_{1,2} & y_{1,2} & \Delta t_{1,2} \\ x_{1,3} & y_{1,3} & \Delta t_{1,3} \\ x_{1,4} & y_{1,4} & \Delta t_{1,4} \end{bmatrix} \begin{Bmatrix} x_I \\ y_I \\ {V_g}^2 t_1 \end{Bmatrix} = \frac{1}{2} \begin{Bmatrix} b_2 \\ b_3 \\ b_4 \end{Bmatrix} - \frac{{V_g}^2}{2} \begin{Bmatrix} {\Delta t_{1,2}}^2 \\ {\Delta t_{1,3}}^2 \\ {\Delta t_{1,4}}^2 \end{Bmatrix} \tag{14}$$

or, in general, (14) can be written as:

$$[A]\{\boldsymbol{x}\} = \{B\} - {V_g}^2 \{C\} \tag{15}$$

The expression for $\{\boldsymbol{x}\}$ vector is:

$$\{\boldsymbol{x}\} = [A]^{-1}\{B\} - {V_g}^2 [A]^{-1}\{C\} \tag{16}$$

Considering $a_i = [A]^{-1}\{B\}|_i$ and $c_i = [A]^{-1}\{C\}|_i$, we achieve:

$$\begin{Bmatrix} x_I \\ y_I \\ {V_g}^2 t_1 \end{Bmatrix} = \begin{Bmatrix} a_1 \\ a_2 \\ a_3 \end{Bmatrix} - {V_g}^2 \begin{Bmatrix} c_1 \\ c_2 \\ c_3 \end{Bmatrix} \tag{17}$$

so that the following expressions for the four unknowns are obtained:

$$\begin{cases} x_I = a_1 - {V_g}^2 c_1 \\ y_I = a_2 - {V_g}^2 c_2 \\ {V_g}^2 t_1 = a_3 - {V_g}^2 c_3 \end{cases} \tag{18}$$

Substituting expressions (18) into the reference sensor equation of (9), after mathematical manipulation a third order equation with t_1 as unknowns is formulated. This is:

$${t_1}^3 k_1 + {t_1}^2 k_2 + t_1 k_3 + k_4 = 0 \tag{19}$$

Although (19) is a third order equation, only one solution is feasible, whereas the other two should be discarded. After obtaining t_1 from (19), V_g can simply be calculated using the following equation:

$$V_g = \sqrt{\frac{a_3}{t_1 + d_3}} \tag{20}$$

Impact coordinates are then calculated from (18).

6 EXPERIMENTAL SET-UP

Three low velocity impacts conducted on an aluminium plate with dimensions $350\,mm$

long, 260 mm wide and 9 mm thick were investigated.

The impacts were generated using a hand-held modal hammer and were measured employing four surface-bonded APC 850 transducers, connected by low-noise cables.

The signals were acquired using a four-channel oscilloscope with 16 bits of resolution, a sampling rate of 20 MHz and an acquisition window of 5 ms. Both systems were synchronized in way that all the transducers were triggered by one of the sensors (reference sensor).

A MATLAB software code, implemented by the authors, was written to analyse the waveforms for finding the TOAs and the impact location. Firstly, the data were filtered numerically by a 4th-order Butterworth band-pass filter. Sensors location and impact source coordinates are reported in

Table 1 and Table 2. A sketch of the experimental set-up, sensor arrangements and impacts location are presented in

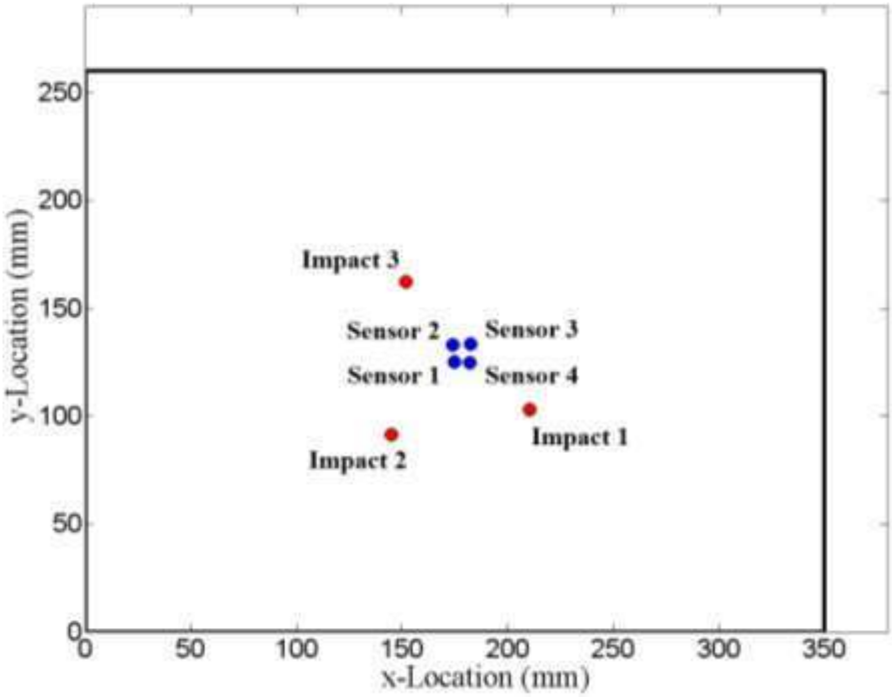

. The waveforms of the acquired signals for Impact 1 are shown in Figure2

	Sensor 1	Sensor 2	Sensor 3	Sensor 4 (ref)
x-Coordinate (mm)	175	174	182.6	182.3
y-Coordinate (mm)	125	133	133.5	124.6

Table 1: Sensor coordinates

	Impact 1	Impact 2	Impact 3
x-Coordinate (mm)	210.66	145	151.95
y-Coordinate (mm)	102.86	91.45	162.26

Table 2: Impact source coordinates

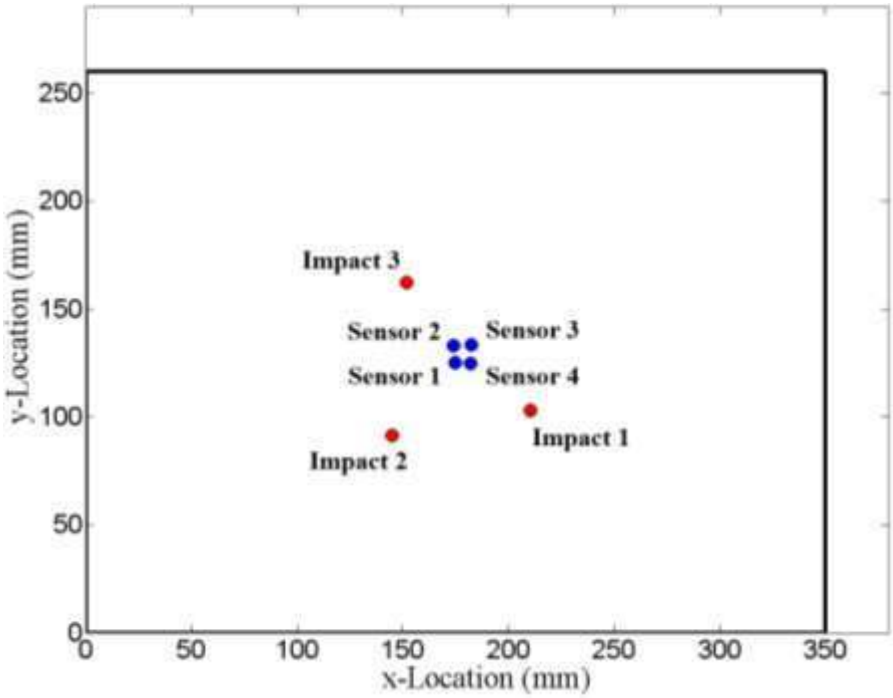

Figure 1: Sensors and impacts location on considered aluminium plate

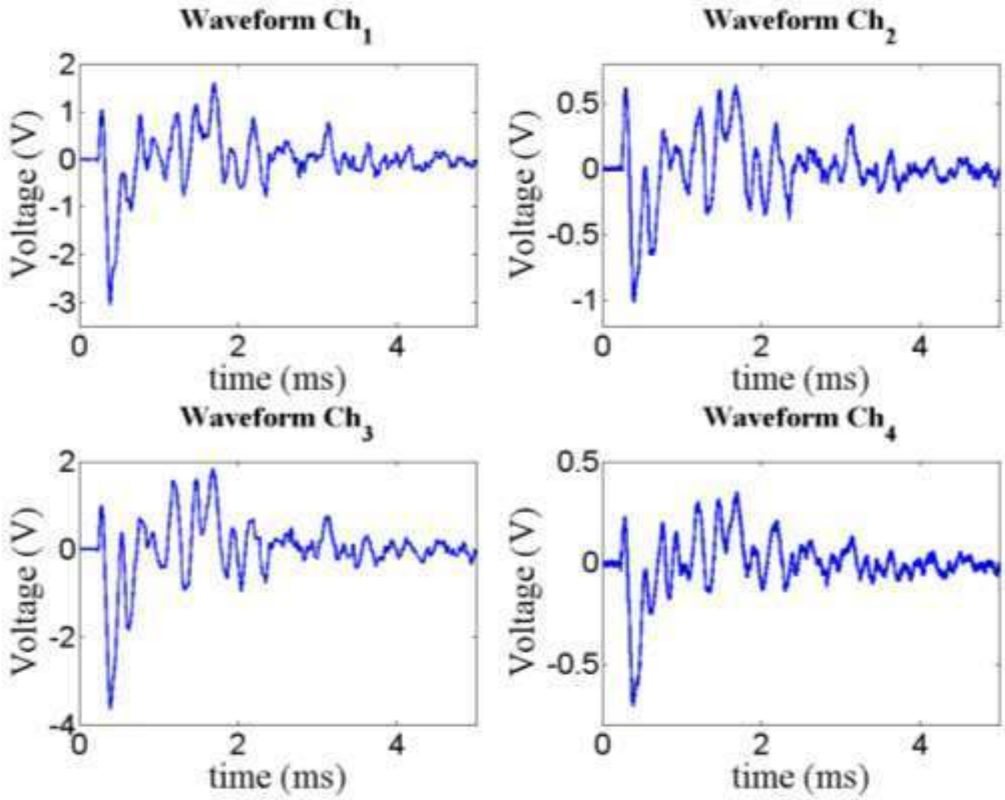

Figure 2: Acquired signals during Impact 1

6 RESULTS

Results of the application of the first ToA method (i.e. the two-step AIC pickers, see Section 3) on the acquired signal 1 in Impact 1 are presented in Figure 3.

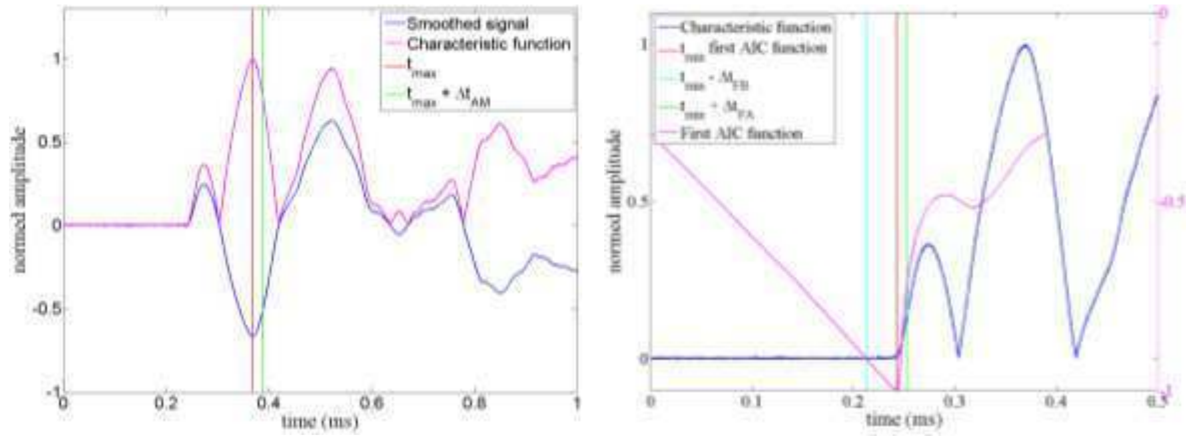

(a) (b)

Figure 3: Visual description of the two-step AIC pickers (method 1): (a) determination of the initial time window, (b) first step of the method with determination of the new time window

Time of arrivals, calculated by using the first method in Impact 1, are presented in Figure 4 on the initial part of the four signals.

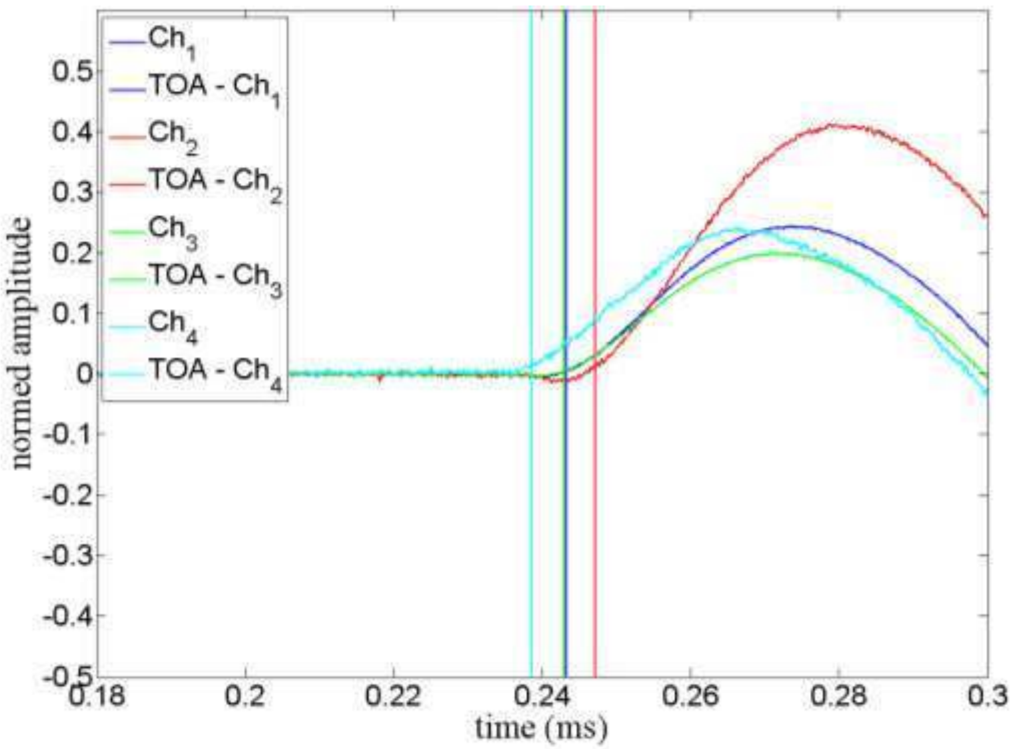

Figure 4: ToAs calculated by using the first method in Impact 1

A comparison among ToAs and TDOAs, obtained by using both methods in Impact 1, are reported in Table 3 and Table 4.

	Sensor 1	Sensor 2	Sensor 3	Sensor 4
Method 1 – ToA (ms)	0.2433	0.2472	0.2429	0.2386
Method 2 – ToA (ms)	0.2431	0.2472	0.2426	0.2383

Table 3: ToAs comparison in Impact 1

	$TOA\,1 - TOA\,4$	$TOA\,2 - TOA\,4$	$TOA\,3 - TOA\,4$
Method 1 – TDOAs (ms)	0.0047	0.0086	0.00435
Method 2 – TDOAs (ms)	0.0048	0.0089	0.0043

Table 4: TDOAs comparison in Impact 1

Figure 5 shows the results of the impact localization algorithm considering the two methods, whilst table 5 reports the evaluated impact positions and the errors as expressed by the following formula:

$$\psi = \sqrt{(x_{real} - x_{calculated})^2 + (y_{real} - y_{calculated})^2} \tag{23}$$

where (x_{real}, y_{real}) are the coordinates of the real impact position and $(x_{calculated}, y_{calculated})$ are the coordinates of the impact location using the algorithms reported in Sections 3 and 4.

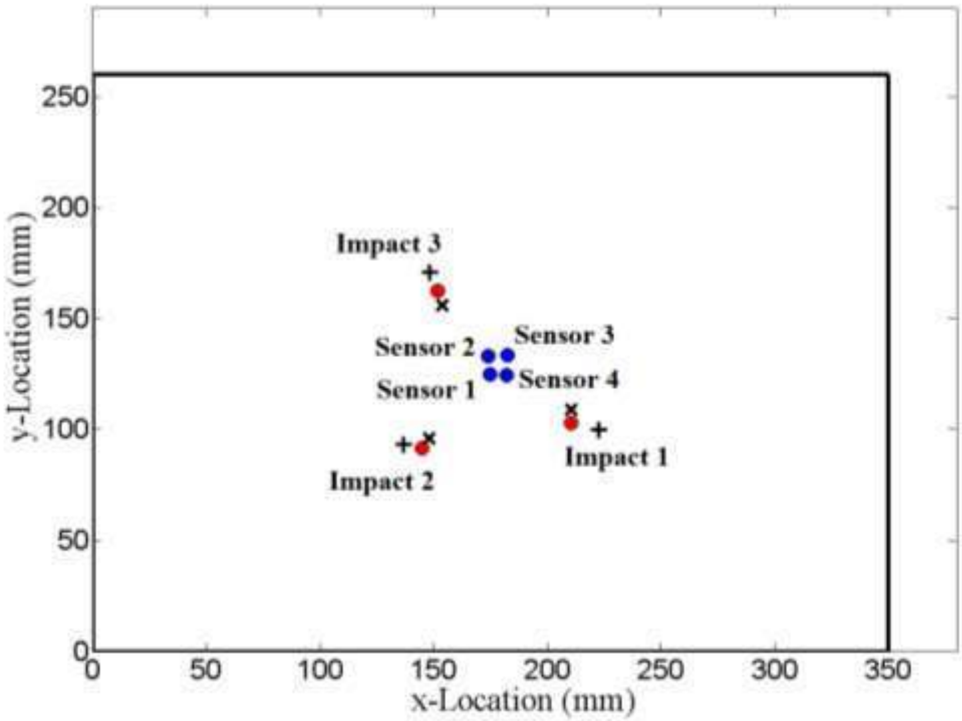

Figure 5: Source location results: by using the first method (x) and the second method (+)

Impact 1	x-Coordinate source location (mm)	y-Coordinate source location (mm)	Location error ψ (mm)
Real value	210.6	102.8	
Algorithm 1	210.5	108.8	5.97
Algorithm 2	222.9	99.6	12.71
Impact 2			
Real value	145	91.45	
Algorithm 1	148.22	95.95	5.52
Algorithm 2	136.91	93.05	8.26
Impact 3			
Real value	151.95	162.26	
Algorithm 1	153.95	155.96	6.61
Algorithm 2	148.56	179.56	8.96

Table 5: Source location results

7 CONCLUSIONS

A new linearized algorithm for AE source localization is presented and investigated. TDOAs information is obtained as differences of TOAs calculated by using two different AIC techniques. Experiments are performed on an aluminium plate with four piezoelectric transducers surface-bonded in a very close geometric configuration. The output of the implemented algorithm are the impact coordinates and the velocity of the stress waves reaching the sensors. A comparison among the results obtained by using the two AIC pickers is performed. These results show the validity of the linearization approach. Furthermore they demonstrate how much accurate the information about TDOAs has to be (i.e. less than 0.0048 ms for a localisation error of 5.5 mm). Future work is ongoing to test the validity of the described approach on a composite plate-like structure, for both application of AIC pickers and the linearization approach of nonlinear equations.

REFERENCES

[1] Tobias, Acoustic emission source location in two dimensions by an array of three sensors. Nondestruct Test, **9**, 9-12, 1976.

[2] F. Ciampa, M. Meo, Acoustic emission source localization and velocity determination of the fundamental mode A_0 using wavelet analysis and Newton-based optimization technique. Impact localization in composite structures of arbitrary cross section. Smart Materials and Structures, **19**, 1-14, 2010.

[3] P. Sedlak, Y. Hirose, M. Enoki, Acoustic emission localization in thin multi-layer plates using first-arrival determination. Mechanical System and Signal Processing, **36**, 636-649, 2013.

[4] J. Kurtz, CU Grosse, Strategies for reliable automatic onset time picking of acoustic emission and of ultrasound signals in concrete. Ultrasonics, **43**, 538-546. 2005.

[5] H. Akaike, Information theory and an extension of the maximum likelihood principle. In: BN Petrov, F Csaki, editors, Second international symposium on information theory, Springer-Verlag, 267-281, 1973.

[6] M. Leonard, BLN Kennett, Multi-component autoregressive techniques for the analysis of seismograms. Physics of the Earth and Planetary Interiors, **113**, 247-263, 1999.

[7] R. Sleeman, T. van Eck, Robust automatic P-phase picking: an on-line implementation in the analysis of broadband seismogram recordings. Physics of the Earth and Planetary Interiors, **113**, 265-275, 1999.

[8] H. Zhang, C. Thurber, C. Rowe, Automatic p-wave arrival detection and picking with multiscale wavelet analysis for single component recordings. Bulletin of the Seismological Society of America, **93** (5), 1904-1912, 2003.

[9] N. Maeda, A method for reading and checking phase times in auto-processing system of seismic wave data, Zisin=Jishin, **38**, 365-379, 1985.

[10] R. Allen, Automatic phase pickers: their present use and future prospects. Bulletin of the Seismological Society of America, **72**, 225-242, 1982.

[11] A. Carpinteri, J. Xu, G. Lacidogna, A. Manuello, Reliable onset time determination and source location of acoustic emissions in concrete structures. Cement & Concrete Composites, **34**, 529-537, 2012.

[12] G. Niccolini, J. Xu, A. Manuello, G. Lacidogna, A. Carpinteri, Onset time determination of acoustic and electromagnetic emission during rock fracture. Progress In Electromagnetics Research Letters, **35**, 51-62, 2012.